Journal of Dental Sciences 19 (2024) 945–951

Available online at www.sciencedirect.com

ScienceDirect

journal homepage: www.e-jds.com

Original Article

Post-polymerization of three-dimensional printing resin using a dental light curing unit

Ryan Jin Young Kim [a†], Dong-Hwan Kim [b†], Deog-Gyu Seo [c*]

[a] *Department of Dental Science, Dental Research Institute, Seoul National University School of Dentistry, Seoul, Republic of Korea*
[b] *Seoul Gospel Dental Clinic, Seoul, Republic of Korea*
[c] *Department of Conservative Dentistry, Dental Research Institute, Seoul National University School of Dentistry, Seoul, Republic of Korea*

Received 23 June 2023; Final revision received 24 July 2023
Available online 7 August 2023

KEYWORDS
Biaxial flexural strength;
Microhardness;
Light curing unit;
Post-polymerization;
Three-dimensional printing

Abstract *Background/Purpose:* In vat photopolymerization, post-polymerization of the three-dimensional (3D) printing resin is necessary to ensure the optimum physical properties of the printed objects. This study aimed to evaluate the potential use of a handheld polywave light-emitting diode (LED) dental light-curing unit (LCU) for post-polymerizing 3D printed resins by measuring the microhardness and biaxial flexural strength of the post-polymerized resin.
Material and methods: 3D printed 1- and 2-mm-thick disks were irradiated with a dental LCU at 3200 mW/cm^2. Post-polymerization was repeated either on one side from the top surface: two cycles (T2), four cycles (T4), and eight cycles (T8), or on both sides from the top and bottom surfaces: one cycle (T1B1), two cycles (T2B2), and four cycles (T4B4) for each side. The microhardness and biaxial strength of the disks were compared to those post-polymerized by a conventional desktop polymerizing unit (PC) and those without post-polymerization (NC).
Results: Microhardness of the disks varied between the top and bottom surfaces of the 1-mm and 2-mm-thick disks, depending on the post-polymerization methods. T8 and T4B4 produced comparable microhardness on the top surface to PC for both thicknesses. In contrast, PC, T2B2, and T4B4 exhibited the highest microhardness on the bottom surface. Except for NC, the 1-mm-thick disks had a higher biaxial flexural strength than the 2-mm-thick disks. T4B4 resulted in the highest biaxial flexural strength for both thicknesses, which was comparable to that of the desktop polymerizing unit.
Conclusion: The microhardness and biaxial flexural strengths of the post-polymerized 3D-printed disks increase with polymerization time. With sufficient polymerization from both

* Corresponding author.
E-mail address: dgseo@snu.ac.kr (D.-G. Seo).
† These authors (Ryan Jin Young Kim and Dong-Hwan Kim) contributed equally to this work.

https://doi.org/10.1016/j.jds.2023.07.028

sides, the polywave LCU has the potential to be a viable alternative to desktop polymerization units.

Introduction

Three-dimensional (3D) printing is an additive manufacturing (AM) process using a bottom-up approach that builds up a 3D object by photopolymerizing or depositing material layer by layer.[1–3] In contrast, a subtractive manufacturing (SM) process uses a computer numeric-controlled machine to mill prefabricated blocks or disks into the desired form using a top-down approach.[3,4] Despite the high quality and dimensional stability of prefabricated materials, SM processes typically generate unnecessary waste and cannot reproduce complex geometries. AM, which is also capable of mass production, can be used to overcome the drawbacks of SM.[1–3]

With the advancement of technologies, material development, and reduction in the cost of use, 3D printing has found wide application in several fields. In dentistry, it has been used to fabricate physical models from digital scans, orthodontic appliances, occlusal splints, surgical guides, and restorations.[1,5–7] Stereolithography apparatus (SLA) and digital light projection (DLP), also known as vat photopolymerization, are the most commonly used 3D printing technologies in dentistry.[8,9] Both technologies use light to build layers by activating the polymerization reaction of photoinitiators for cross-linking monomers and oligomers to form a polymer network of solid resin.[10] Post-processing is required for 3D-printed products to rinse away unpolymerized liquid resin. Post-polymerization at a specific wavelength using a desktop ultraviolet (UV) light polymerizing machine is needed to convert the under-polymerized product in a green state to definitive products.[11] Traditional post-polymerization necessitates the use of a desktop polymerization unit, which can take several minutes to an hour to attain their definitive properties, depending on the 3D printed material and the light intensity of the polymerizing unit.[11,12]

A dental light-curing unit (LCU) has become an essential piece of equipment in everyday dental practice to photopolymerize a variety of photopolymerizable resin-based materials for direct and indirect restorative treatments.[13] Conventional LCUs have the peak absorption spectrum of camphorquinone, the most commonly used photoinitiator in composite resins. Conversely, third-generation light-emitting diode (LED) LCUs have been developed to optimally activate various photoinitiators incorporated in different resin-based materials because not all resin-based materials use the same photoinitiators.[14] Theoretically, the broad wavelength range of polywave LCUs would be able to activate the photoinitiators used in vat photopolymerization. However, no studies have yet been conducted to assess the use of dental LCUs in the post-polymerization of 3D-printed objects. Therefore, this study aimed to evaluate the potential use of a handheld polywave LED dental LCU for post-polymerizing 3D printed resin by measuring the microhardness and biaxial flexural strengths compared to conventional desktop post-polymerizing units. The null hypothesis was that there would be no difference in the microhardness and biaxial flexural strength of post-polymerized 3D printed resin between the desktop post-polymerizing unit and dental LCU, regardless of the disk thickness or irradiation time of the dental LCU.

Materials and methods

Specimen preparation

Disks with a 2 cm diameter and 1- or 2-mm thick were designed (Rhino 3D; Robert McNeel & Associates, Seattle, WA, USA) and fabricated using a 3D printer (Zenith L2; Dentis, Daegu, Korea) using a 3D printing photopolymerizable resin for crown and denture teeth fabrication (ZMD-1000B C&T shade A3; Dentis). The disks were printed with a layer thickness of 100 μm in a 0-degree orientation parallel to the build platform. After printing, the unpolymerized resin on the disks was removed by washing for 10 min with ethanol contained in a washer (Anycubic Wash & Cure; Anycubic, Shenzhen, China), and the disks were assigned to one of eight subgroups according to the post-polymerization methods shown in Fig. 1. Negative control (NC) without post-polymerization was used as a baseline. Positive control (PC) was post-polymerized for 7 min using a desktop polymerizing unit (Cure Box; ODS, Incheon, Korea). Six subgroups were post-polymerized only from the top surface or both from the top and bottom surfaces of the disks for a varying number of polymerziation cycles using a polywave handheld LCU (Valo curing light; Ultradent Products, South Jordan, UT, USA). A 405-nm light source was used in both the 3D printer and desktop post-polymerization unit. In the desktop post-polymerization group, positive control (PC), the disks were placed on a rotating plate on the floor of the desktop unit, and the surfaces of the disk facing toward and away from the plate were designated the bottom and top surfaces, respectively. The handheld LCU, which emits broad-spectrum light at 385—515 nm, was used to post-polymerize the 3D printed disks at different cycle exposures, either from one or both sides. The polymerization light was set to the Xtra Power mode (3200 mW/cm^2) for 3 s for each cycle. All post-cured disks were kept in a distilled water bath at 37 °C for 24 h prior to the microhardness and biaxial flexural strength tests.

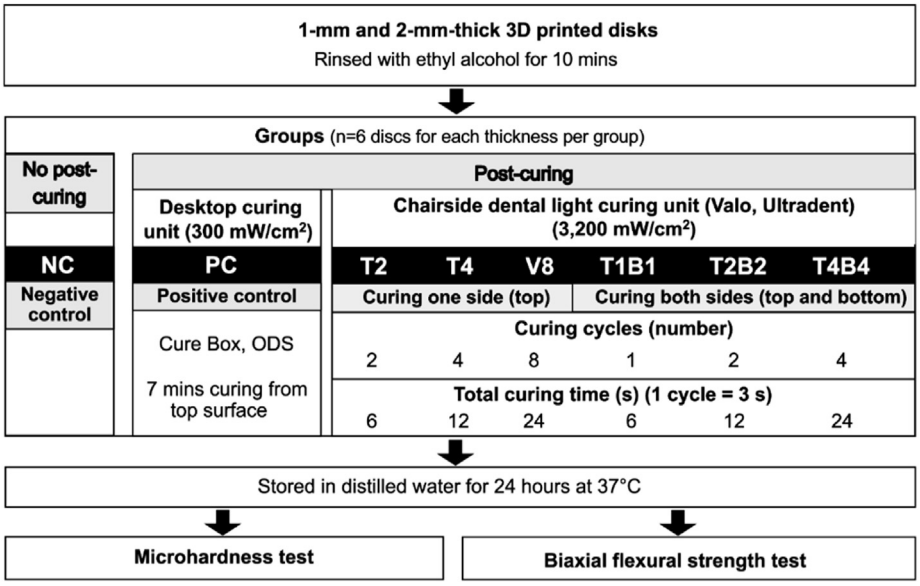

Figure 1 Experimental design.

Microhardness measurement

Following a 24-h storage period, the bottom and top surfaces of the disks from each group were serially wet-polished with 800-, 1200-, 1500-, and 2000-grit silicon carbide abrasive paper (n = 6 per group). Indentations were made on both surfaces of each disk with a load of 0.05 gf for 30 s (HM-200B; Mitutoyo, Kawasaki, Japan). The width and height of each indentation were aligned by using an optical microscope equipped with a testing machine. Three indentations were made on each disk surface and averaged to determine the Vickers hardness of each specimen (HV) using the formula: VHN = $1854.4(P/d^2)$, where P is the load in grams and d is the mean diagonal of indentation in millimeters. The Vickers hardness was determined using the AVPAK software (Mitutoyo) on the instrument.

Biaxial flexural strength measurement

The biaxial flexural strength was measured using a piston-on 3-ball test according to ISO 6872. The disk specimens were placed on three metal spheres, each with a 3.2 mm diameter, and spaced such that there was an angle of 120° between the balls. The distance between the center of the specimen and each metal ball was 6 mm. Biaxial flexural strength tests were conducted using a universal testing machine (Unitest M1, Testone, Siheung, Korea), where the load was applied at a constant speed of 1 mm/min with a 1-mm diameter flat end loading tip until fracture occurred. The failure load was converted from Newton to MPa using the following equation:

$$\text{Biaxial flexural strength} = -0.2387P(X-Y)/d^2;$$

$$X = (1+\nu)\ln(r_2/r_3)^2+[(1-\nu)/2](r_2/r_3)^2,\ Y = (1+\nu)[1+\ln(r_1/r_3)^2]+(1-\nu)(r_1/r_3)^2,$$

where P is the total load causing fracture (N), ν is Poisson's ratio (0.24), r_1 is the radius of the support circle (6 mm), r_2 is the radius of the loaded area (0.5 mm), r_3 is the radius of the specimen (10 mm), and d is the thickness of the specimen at the fracture origin (1 or 2 mm).

Statistical analysis

Statistical analyses were performed using IBM SPSS Statistics, v25 (IBM, Armonk, NY, USA). Levene's test confirmed the equality of variance, and the Shapiro–Wilk test verified each variable's normality. One-way ANOVA was performed to analyze the test values of the 3D disks, followed by Tukey's Honest Significant Difference post-hoc test, and an independent t-test was used to compare the values between the 1- and 2-mm-thick disks ($\alpha = 0.05$).

Results

The microhardness of the disks varied between 1- and 2-mm-thick disks and between the top and bottom surfaces, depending on the post-polymerization method (Table 1 and Fig. 2A and B). The microhardness values of the top surface in both 1- and 2-mm-thick disks were highest in T4B4 and T8 ($P < 0.05$), which were comparable to those of the PC ($P > 0.05$). PC, T2B2, and T4B4 showed the highest microhardness on the bottom surface for both thicknesses ($P < 0.05$). However, the values were significantly lower on the bottom surface when the disks were post-polymerized only from the top surface: this was more pronounced for the 2-mm-thick disks than the 1-mm-thick disks ($P < 0.05$). In the LCU groups, the microhardness values of the top surface increased with the number of post-polymerization cycles for both disk thicknesses. The hardness of the bottom surface was significantly higher in T4 than that in T2 ($P < 0.05$), but there was no significant difference between T4 and T8 ($P > 0.05$).

In the LCU groups, the biaxial flexural strength showed a tendency to increase with the number of polymerization

Table 1 Microhardness of top and bottom surfaces of (A) 1-mm and (B) 2-mm-thick disks.

	A									
	NC	PC	T2	T4	T8	T1B1	T2B2	T4B4	*F*	*P*
Top	5.57 (1.43) D	23.29 (1.00) A	17.93 (0.80) C*	19.78 (0.62) BC*	22.51 (0.80) A*	18.63 (0.52) C	19.53 (0.96) BC	21.37 (2.20) AB	115.634	<0.001
Bottom	5.04 (0.79) f	22.95 (1.34) a	6.55 (0.69) f	16.93 (1.54) de	15.86 (1.59) e	19.94 (1.24) bc	20.68 (0.76) abc	21.65 (1.50) ab	138.428	<0.001
t	0.783	0.533	26.422	4.227	9.304	−2.354	−2.297	−0.230		
P	0.452	0.605	<0.001	0.002	<0.001	0.051	0.055	0.823		
	B									
	NC	PC	T2	T4	T8	T1B1	T2B2	T4B4	*F*	*P*
Top	6.63 (0.67) C	23.65 (1.20) A	18.34 (0.81) B*	19.32 (1.09) B*	20.89 (1.30) AB*	19.17 (0.52) B	19.35 (0.68) B	20.74 (2.42) AB	79.570	<0.001
Bottom	6.90 (0.64) f	23.10 (0.78) a	6.93 (0.66) f	13.98 (1.08) c	13.40 (1.50) c	20.01 (0.74) b	20.18 (0.71) ab	22.19 (2.04) ab	171.093	<0.001
t	−0.745	0.930	27.041	8.586	9.173	−2.349	−2.183	−1.123		
P	0.474	0.374	<0.001	<0.001	<0.001	0.053	0.060	0.288		

F, F-value; *t*, t-value; *P*, p-value.
NC, negative control (no post-polymerization); PC, positive control (conventional post-polymerization unit).
T2, T4, T8 represented groups subjected to 2, 4, and 8 cycles of post-polymerization on one side from the top surface, respectively.
T1B1, T2B2, T4B4 represented groups subjected to 1, 2, and 4 cycles of post-polymerization on both sides from the top and bottom sufaces, respectively.
Different uppercase and lowercase letters indicate statistically significant differences between groups on the top and bottom surfaces, respectively (one-way ANOVA, Tukey HSD post-hoc, $P < 0.05$).
Asterisks indicate statistically significant differences between the top and bottom surfaces within the same group (independent *t*-test, $P < 0.05$).

cycles, and when both sides were post-polymerized rather than irradiated on a single side irradiation for the same number of polymerization cycles (T2 vs. T1B1; T4 vs. T2B2; T8 vs. T4B4), but a significantly higher value was observed in T4B4 than in T8 ($P < 0.05$) (Table 2 and Fig. 3). Except for NC, the 1-mm-thick disks had a higher biaxial flexural strength than the 2-mm-thick disks. Overall, T4B4 had the highest biaxial flexural strength for both thicknesses ($P < 0.05$), which was comparable to that of the PC ($P > 0.05$).

Discussion

This study evaluated the potential use of a chairside polywave LCU to post-polymerize 3D-printed resin compared to conventional desktop post-polymerization units by analyzing the microhardness and biaxial flexural strength of 3D-printed post-processed disks. The findings of this study do not support the null hypothesis that the microhardness and biaxial flexural strength of post-polymerized 3D-printed resin would not differ between the conventional desktop post-polymerization unit (PC) and dental LCU (Valo) because the values varied depending on the disk thickness and irradiation time.

The post-polymerization time in 3D printing varies depending on the photopolymer and polymerizing machine used.[11,12] In vat photopolymerization, the degree of polymerization and post-polymerization process influence the mechanical properties of the 3D-printed object.[11,15,16] During composite resin restoration, clinicians are advised to position the tip of the LCU as close to the resin material as possible[13,17–20] because adequate photo polymerization is essential for the long-term integrity of the 3D-printed parts. However, unlike dental LCUs, the distance between the light source and the object being cured is not easily controlled with a desktop post-polymerization unit with multiple LED lamps positioned on the inner walls of the polymerization chamber. Therefore, chairside dental LCUs have the advantage of being portable devices that are readily available in every dental clinic and could thus be potentially used in the post-polymerization of 3D printed parts as long as the mechanical properties of the post-cured 3D printed resin are comparable to those post-cured by conventional desktop units. In addition to being portable devices that can be easily manipulated to the object being polymerized, the light intensity of dental LCUs is generally higher, theoretically reducing the overall polymerization time compared to conventional post-polymerization units.

The microhardness test is a well-established method for determining the degree of conversion.[21,22] In this study, the microhardness increased significantly upon light activation. Even after a brief post-polymerization period using the LCU, the microhardness values of the photopolymerized surface were comparable to or slightly lower than those of the desktop post-polymerization unit. The number of post-polymerization cycles in the LCU groups had no marked effect on the hardness when both sides of the disks were post-polymerized, regardless of the disk thickness. However, when the disks were post-polymerized only from the top surface, the microhardness values of the bottom surface were significantly lower, particularly in the 2-mm-

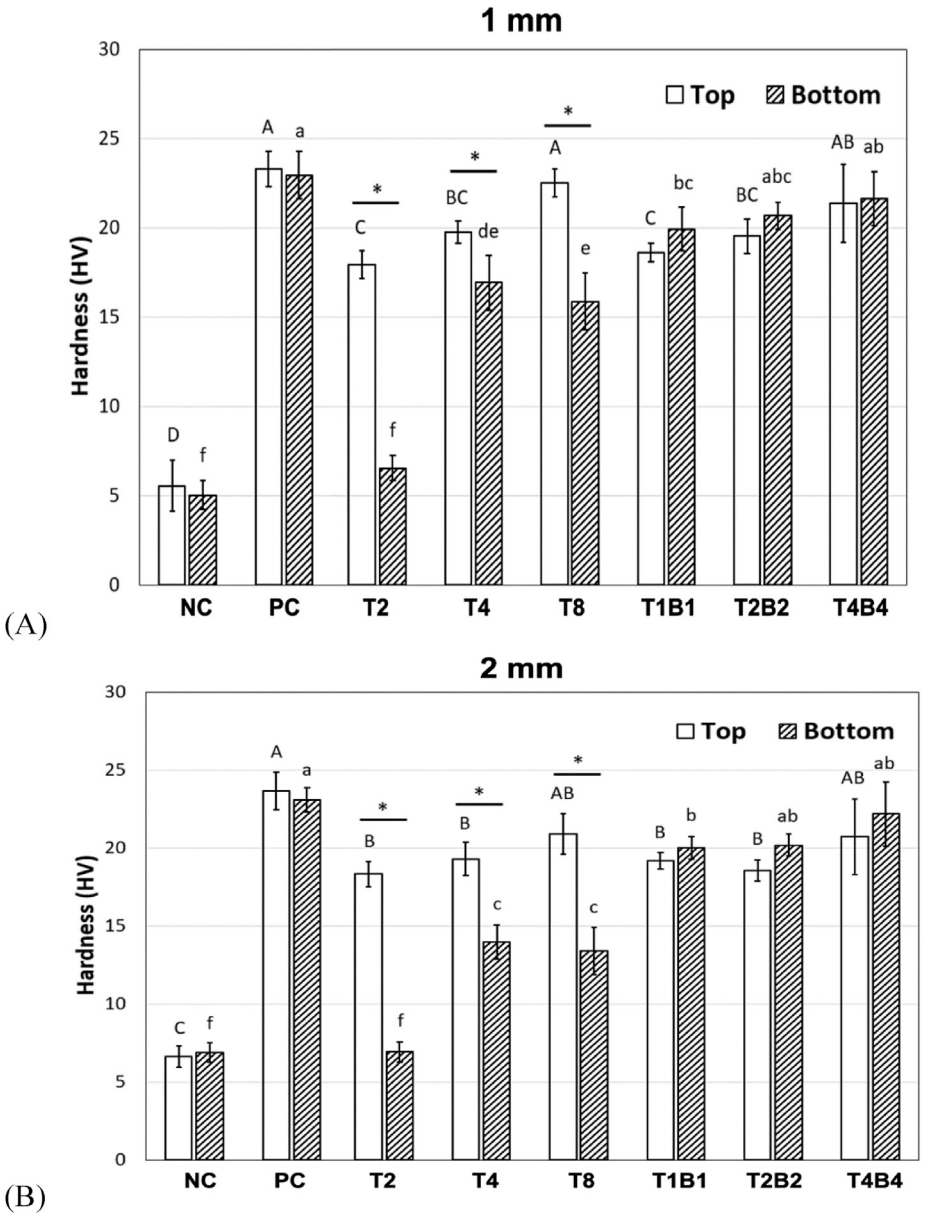

Figure 2 Microhardness of top and bottom surfaces of (A) 1-mm and (B) 2-mm-thick disks. NC, negative control (no post-polymerization); PC, positive control (conventional post-polymerization unit). T2, T4, T8 represented groups subjected to 2, 4, and 8 cycles of post-polymerization on one side from the top surface, respectively. T1B1, T2B2, T4B4 represented groups subjected to 1, 2, and 4 cycles of post-polymerization on both sides from the top and bottom sufaces, respectively. Different uppercase and lowercase letters indicate statistically significant differences between groups on the top and bottom surfaces, respectively ($P < 0.05$). Asterisks indicate statistically significant differences between the top and bottom surfaces within the same group ($P < 0.05$).

thick disks compared to the 1-mm-thick disks, unless post-polymerized multiple times. The results show that while light activation can produce acceptable superficial microhardness, light is rapidly attenuated within the resin and will not sufficiently polymerize it without an adequate light activation.

The biaxial flexural strength test supports the need for longer light activation times in the LCU. The difference in biaxial flexural strength values between the LCU and conventional post-polymerization units was not statistically significant after multiple light-curing cycles, indicating that a dental LCU could potentially be used in the post-polymerization of 3D printed objects. The biaxial flexural strength of the 1-mm-thick disk was greater than that of the 2-mm-thick disk. This difference implies that light transmission decreases with thickness, influencing the definitive physical properties.[18] Thicker resins would necessitate a longer polymerization time or a higher light intensity to compensate for the light attenuation.[23,24]

The desktop post-curing unit (PC) was operated with the bottom surface of the disk facing the polymerization table, allowing direct light to reach the upper surface. The PC

Table 2 Biaxial flexural strength (MPa) of 1-mm and 2-mm-thick disks.

	NC	PC	T2	T4	T8	T1B1	T2B2	T4B4	*F*	*P*
1 mm	123.71 (7.75) C	196.45 (23.66) A*	146.24 (26.98) BC*	146.98 (13.89) BC*	151.91 (11.61) BC*	157.75 (12.69) BC*	171.13 (18.35) AB*	188.45 (14.14) A*	10.554	<0.001
2 mm	116.39 (6.80) c	170.90 (9.71) a	113.91 (15.28) c	115.37 (11.80) c	136.38 (10.68) bc	118.95 (8.74) c	135.32 (19.16) bc	154.35 (13.53) ab	14.759	<0.001
t	1.738	2.447	2.555	4.249	2.411	6.168	3.306	4.267		
P	0.113	0.034	0.029	0.002	0.037	<0.001	0.008	0.002		

F, F-value; t, t-value; P, p-value.
NC, negative control (no post-polymerization); PC, positive control (conventional post-polymerization unit).
T2, T4, T8 represented groups subjected to 2, 4, and 8 cycles of post-polymerization on one side from the top surface, respectively.
T1B1, T2B2, T4B4 represented groups subjected to 1, 2, and 4 cycles of post-polymerization on both sides from the top and bottom sufaces, respectively.
Different uppercase and lowercase letters indicate statistically significant differences between groups within 1-mm-thick disks and 2-mm-thick disks, respectively (one-way ANOVA, Tukey HSD post-hoc, $P < 0.05$).
Asterisks indicate a statistically significant difference between 1-mm and 2-mm-thick disks within the same group (independent *t*-test, $P < 0.05$).

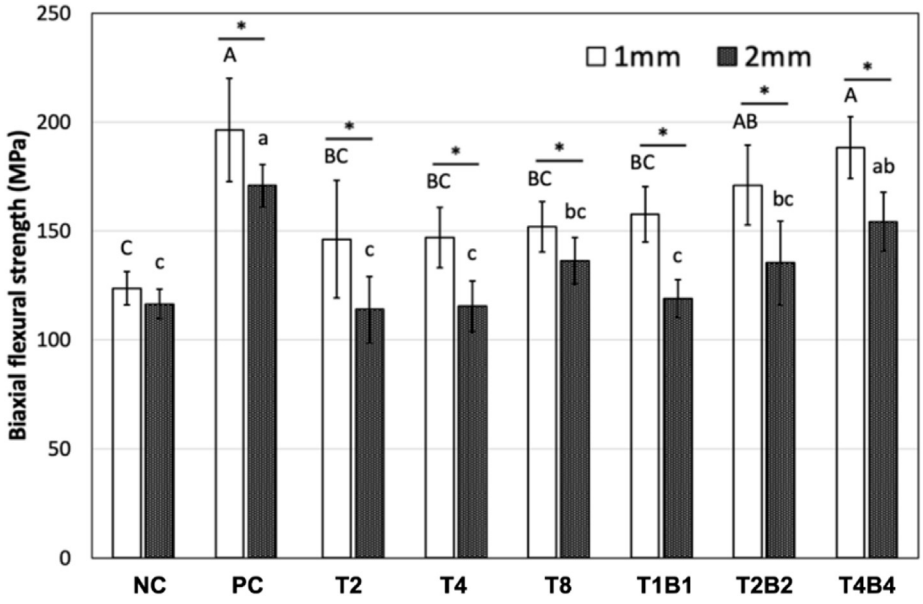

Figure 3 Biaxial flexural strength of 1-mm and 2-mm-thick disks. NC, negative control (no post-polymerization); PC, positive control (conventional post-polymerization unit). T2, T4, T8 represented groups subjected to 2, 4, and 8 cycles of post-polymerization on one side from the top surface, respectively. T1B1, T2B2, T4B4 represented groups subjected to 1, 2, and 4 cycles of post-polymerization on both sides from the top and bottom sufaces, respectively. Different uppercase and lowercase letters indicate statistically significant differences between groups within 1-mm-thick disks and 2-mm-thick disks, respectively ($P < 0.05$). Asterisks indicate a statistically significant difference between the 1-mm and 2-mm-thick disks within the same group ($P < 0.05$).

used multiple UV LEDs with wavelengths ranging from 395 to 405 nm and a maximum light intensity of 300 mW/cm^2. Despite the lower light intensity compared to the investigated chairside LCU, sufficient activating light arrived from multiple directions and resulted in the bottom surface gaining a microhardness similar to that of the top surface. This finding could be attributed to the increased temperature of the polymerization chamber and extended polymerization time from multiple light sources. Previous studies have shown that increasing the temperature during polymerization improves the physical properties.[16,25,26] Heat facilitates the mobility of the polymer network, which aids in bond formation.[12,27] The effect of generated heat from polymerization and LED light sources during the post-curing process on the degree of conversion remains to be assessed.

The handheld dental polymerization light used in this study delivered a broad-spectrum wavelength of 385—515 nm, with three different types of LEDs emitting at 405, 445, and 465 nm. For maximum photopolymerization efficiency, the spectral output of the light source should correspond to the absorption spectrum of the photoinitiator

incorporated in the photopolymerization resin.[28] The photoinitiator used in the 3D printed resin for this study is bis(2,4,6-trimethylbenzoyl)-phenylphosphine oxide, which is one of commonly employed types of photoinitiators for vat polymerization at 405 nm.[29]

Therefore, a limitation of this study was that only one type of dental LCU and a single 3D printing material were used to evaluate the biaxial flexural strength and microhardness compared with a desktop polymerization unit. Since higher light irraditaion intensity may lead to overheating and premature polymerization termination, further studies are warranted to validate the potential application of a polywave dental LCU for post-polymerization 3D printed products. These studies should involve varying the light irradiation conditions with other available dental LCUs with different wavelengths and light intensities. With more research, the application of chairside dental LCU could be a viable portable clinical strategy for post-polymerizing 3D printed products when combined with optimal light properties.

Within the limitations of this study, the microhardness and biaxial flexural strengths of the post-polymerized 3D-printed disks increase with polymerization time. With sufficient polymerization from both sides, the polywave LCU has the potential to be a viable alternative to desktop polymerization units.

Declaration of competing interest

The authors have no conflicts of interest relevant to this article.

Acknowledgements

This work was supported by the National Research Foundation of Korea Grant funded by the Korean Government (MSIT) (No. 2020R1F1A1076307, 2022R1F1A1063198, and 2023R1A2C200786411).

References

1. Dawood A, Marti Marti B, Sauret-Jackson V, Darwood A. 3D printing in dentistry. *Br Dent J* 2015;219:521—9.
2. Kessler A, Hickel R, Reymus M. 3D printing in dentistry-state of the art. *Operat Dent* 2020;45:30—40.
3. van Noort R. The future of dental devices is digital. *Dent Mater* 2012;28:3—12.
4. Reymus M, Lumkemann N, Stawarczyk B. 3D-printed material for temporary restorations: impact of print layer thickness and post-curing method on degree of conversion. *Int J Comput Dent* 2019;22:231—7.
5. Huettig F, Kustermann A, Kuscu E, Geis-Gerstorfer J, Spintzyk S. Polishability and wear resistance of splint material for oral appliances produced with conventional, subtractive, and additive manufacturing. *J Mech Behav Biomed Mater* 2017;75:175—9.
6. Schweiger J, Edelhoff D, Guth JF. 3D printing in digital prosthetic dentistry: an overview of recent developments in additive manufacturing. *J Clin Med* 2021;10:2010.
7. Turbush SK, Turkyilmaz I. Accuracy of three different types of stereolithographic surgical guide in implant placement: an in vitro study. *J Prosthet Dent* 2012;108:181—8.
8. Turkyilmaz I, Wilkins GN. 3D printing in dentistry - exploring the new horizons. *J Dent Sci* 2021;16:1037—8.
9. Ahmad I, Al-Harbi F. *3D Printing in Dentistry 2019/2020*, first ed. London: Quintessence Publishing, 2019:9—18.
10. Pagac M, Hajnys J, Ma QP, et al. A review of vat photopolymerization technology: materials, applications, challenges, and future trends of 3D printing. *Polymers* 2021;13:598.
11. Kim D, Shim JS, Lee D, et al. Effects of post-curing time on the mechanical and color properties of three-dimensional printed crown and bridge materials. *Polymers* 2020;12:2762.
12. Formlabs. An introduction to post-curing SLA 3D prints. Available at: https://formlabs.com/eu/blog/introduction-post-curing-sla-3d-prints. [Date accessed: March 15, 2023].
13. Price RB, Ferracane JL, Hickel R, Sullivan B. The light-curing unit: an essential piece of dental equipment. *Int Dent J* 2020;70:407—17.
14. Jandt KD, Mills RW. A brief history of LED photopolymerization. *Dent Mater* 2013;29:605—17.
15. Al Rashid A, Ahmed W, Khalid MY, Koc M. Vat photopolymerization of polymers and polymer composites: processes and applications. *Addit Manuf* 2021;47:102279.
16. Jindal P, Juneja M, Bajaj D, Siena FL, Breedon P. Effects of post-curing conditions on mechanical properties of 3D printed clear dental aligners. *Rapid Prototyp J* 2020;26:1337—44.
17. Almuallem Z, McDonnell S, Busuttil-Naudi A, Santini A. The effect of irradiation distance on light transmittance and vickers hardness ratio of two bulk-fill resin-based composites. *Eur J Prosthodont Restor Dent* 2016;24:203—14.
18. Rode KM, Kawano Y, Turbino ML. Evaluation of curing light distance on resin composite microhardness and polymerization. *Operat Dent* 2007;32:571—8.
19. Hasanain FA, Nassar HM, Ajaj RA. Effect of light curing distance on microhardness profiles of bulk-fill resin composites. *Polymers* 2022;14:528.
20. Price RB, Felix CA, Andreou P. Effects of resin composite composition and irradiation distance on the performance of curing lights. *Biomaterials* 2004;25:4465—77.
21. Knobloch L, Kerby RE, Clelland N, Lee J. Hardness and degree of conversion of posterior packable composites. *Operat Dent* 2004;29:642—9.
22. Santos GB, Medeiros IS, Fellows CE, Muench A, Braga RR. Composite depth of cure obtained with OTH and LED units assessed by microhardness and micro-Raman spectroscopy. *Operat Dent* 2007;32:79—83.
23. Rodriguez A, Yaman P, Dennison J, Garcia D. Effect of light-curing exposure time, shade, and thickness on the depth of cure of bulk fill composites. *Operat Dent* 2017;42:505—13.
24. Ilday NO, Bayindir YZ, Bayindir F, Gurpinar A. The effect of light curing units, curing time, and veneering materials on resin cement microhardness. *J Dent Sci* 2013;8:141—6.
25. Bayarsaikhan E, Lim JH, Shin SH, et al. Effects of postcuring temperature on the mechanical properties and biocompatibility of three-dimensional printed dental resin material. *Polymers* 2021;13:1180.
26. Tian Y, Chen C, Xu X, et al. A review of 3D printing in dentistry: technologies, affecting factors, and applications. *Scanning* 2021;2021:9950131.
27. Fomlabs. How to post-cure your resin 3D prints. Available at: https://formlabs.com/blog/how-to-post-cure-3d-prints. [Date accessed March 15, 2023].
28. Price RB, Felix CA. Effect of delivering light in specific narrow bandwidths from 394 to 515 nm on the micro-hardness of resin composites. *Dent Mater* 2009;25:899—908.
29. Lai H, Zhu D, Xiao P. Yellow triazine as an efficient photoinitiator for polymerization and 3D printing under LEDs. *Macromol Chem Phys* 2019;220:1900315.